Numerical investigation of SASI through a toy model

Jun'ichi SATO,

Thierry Foglizzo and Sébastien Fromang

(CEA-Saclay)

Introduction

- Hydrodynamic instabilities play an important role in **core-collapse SN**.

  ⇒But its mechanism is still a source of debate.

- **"advective-acoustic cycle (AAC)"**

  (Foglizzo & Tagger 2000; Foglizzo 2001, 2002; Blondin et al. 2003; Burrows et al. 2006; Foglizzo et al. 2007; Ohnishi et al. 2006; Scheck et al. 2008; Yamasaki & Foglizzo 2008)

  ⇒But some alternate interpretations were proposed.
  (Blondin 2005; Blondin & Mezzacappa 2006; Laming 2007)

- It is sometimes difficult to recognize the advective-acoustic mechanism in numerical simulations.

  ⇒We need **a simple models** where its properties are fully understood.

- Foglizzo (2006) suggested a simple model, **toy model**, to understand the SASI mechanism.

Toy model

- The toy model describes the basic properties of **the advective-acoustic instability**.
- This model is simple enough to allow for a deep understanding of **the instability mechanism** at work.
- The simple set up of the toy model can be used as **a benchmark test** for numerical simulations.

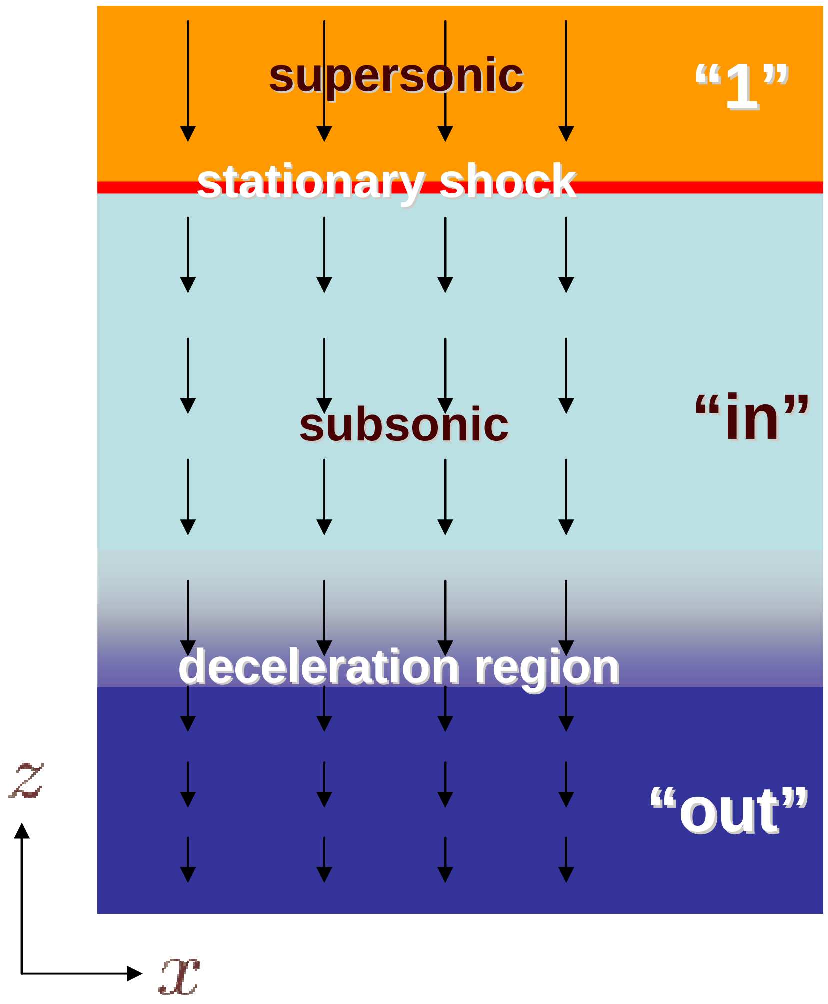

Toy Model

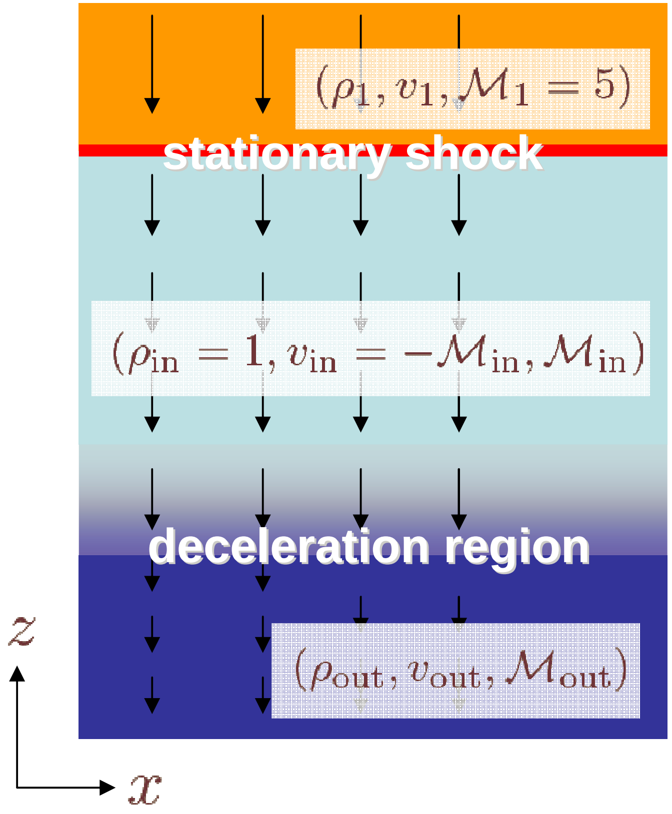

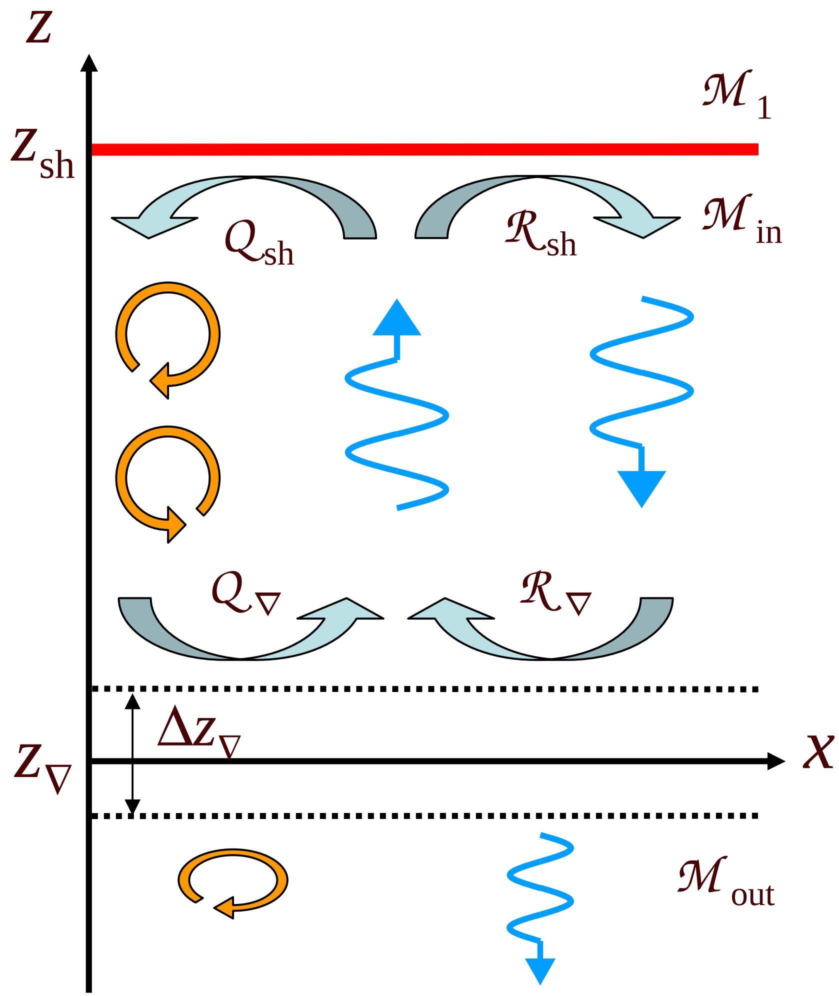

other parameters : $\gamma = \frac{4}{3}, \quad \left(\frac{c_{in}}{c_{out}}\right)^2 = 0.75$

potential : $\Phi(z) = \frac{G\Delta z_\nabla}{2}\left[\tanh\left(\frac{z - z_\nabla}{\Delta z_\nabla/2}\right) + 1\right].$

where $\Delta z_\nabla = 0.1$

Purpose of this work

1. We confirm some behavior of the toy model **using a numerical simulation** and compare to **the linear analysis**.
2. We estimate **the numerical resolution** required in the simulation of the toy model by comparing to the results of the linear analysis.
3. We propose this toy model as **a benchmark test** for SASI simulations.
4. We use this toy model to investigate **the non-linear phase** of SASI.

Numerical Method

- We solve the 1D or 2D Euler equation for inviscid gas.
- Numerical convergence depends on the numerical technique; We use **AUSMDV scheme** (Wada & Liou 1994), which is a **second-order** upwind explicit scheme.

1D advection test (Foglizzo et al. 2005)

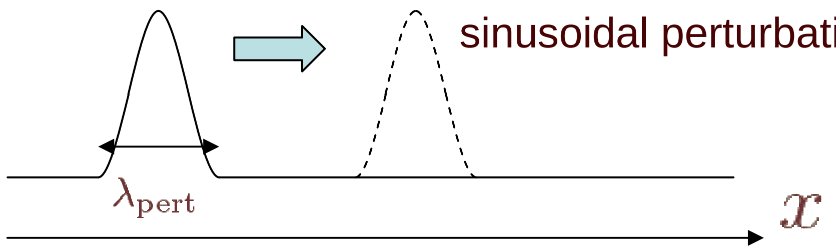

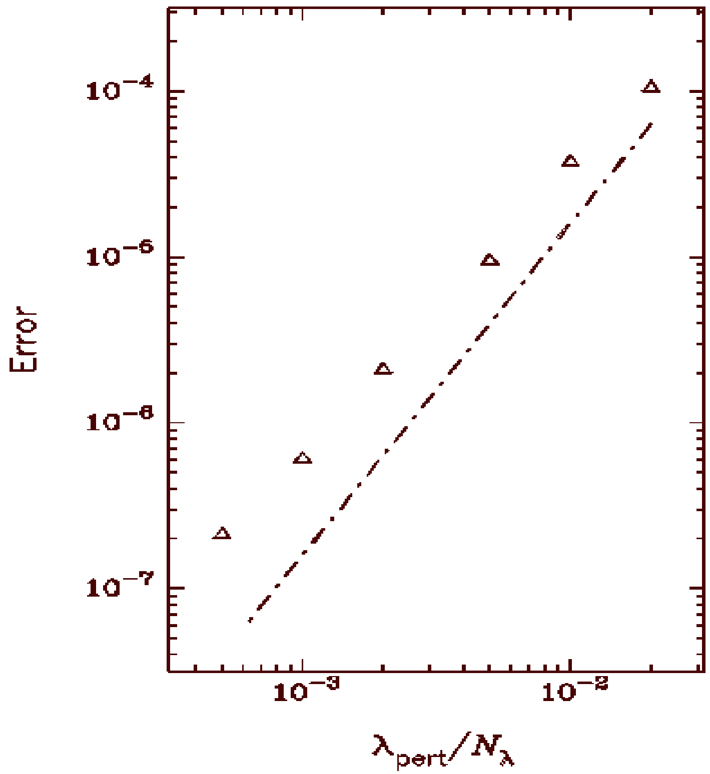

Separated Toy Model

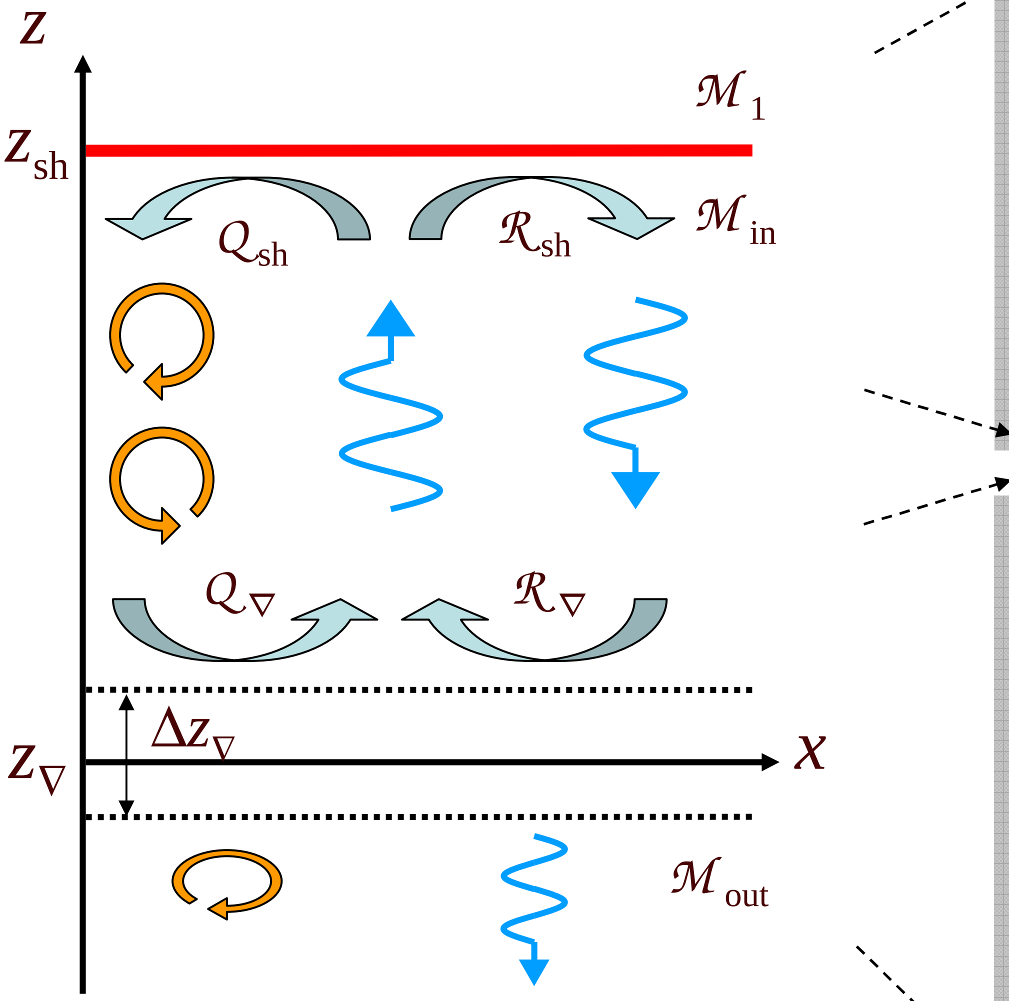

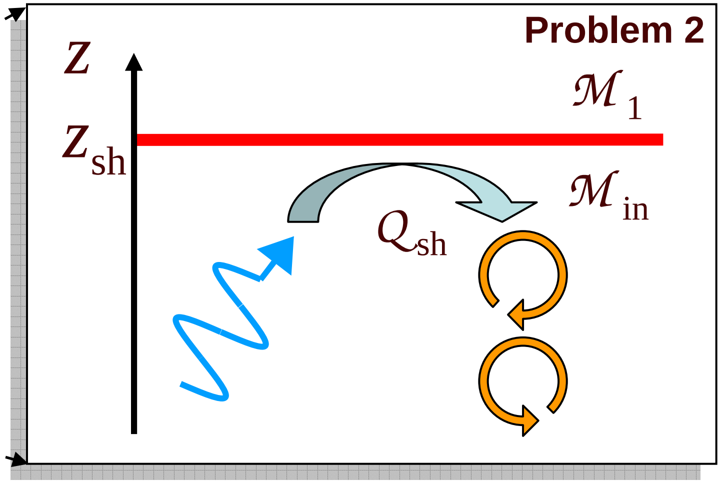

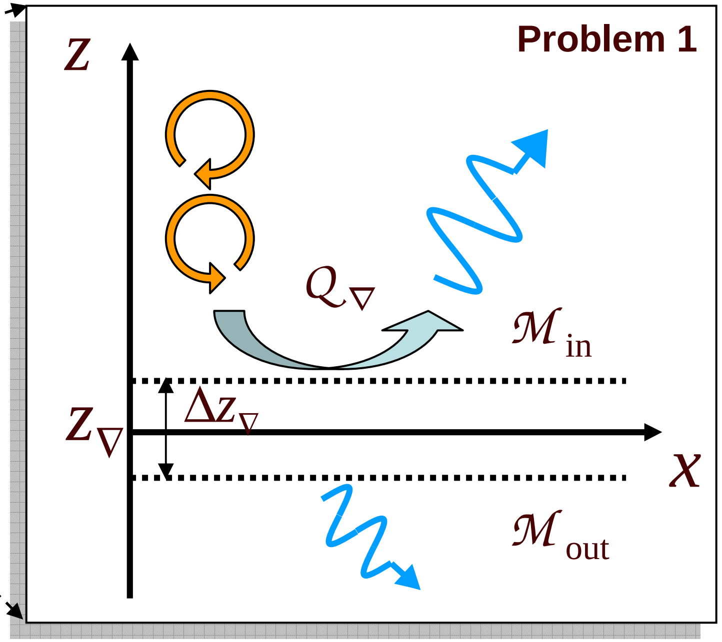

Problem 1

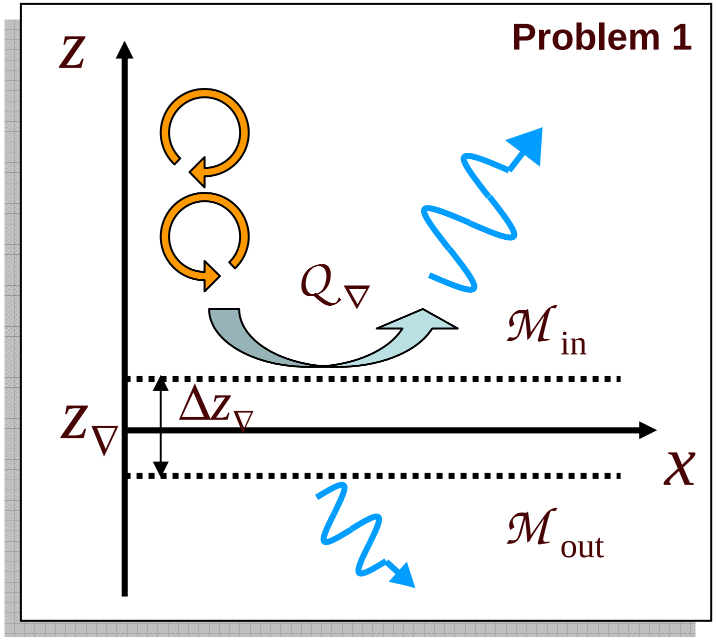

$$\Delta x = 10^{-2}$$
$$\Delta z = 10^{-2}, 10^{-3}, 10^{-4}$$

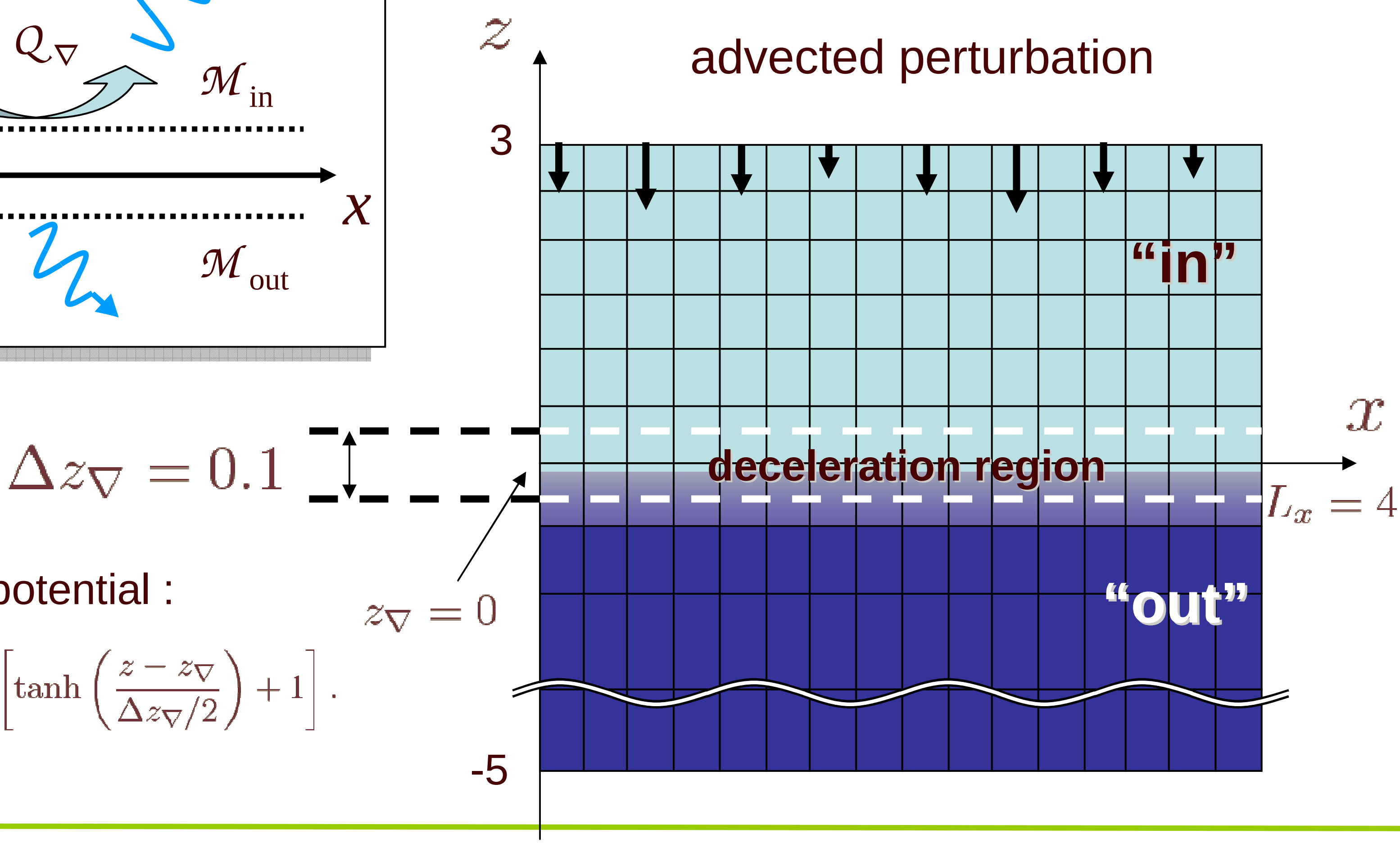

deceleration potential :

$$\Phi(z) = \frac{G\Delta z_\nabla}{2}\left[\tanh\left(\frac{z - z_\nabla}{\Delta z_\nabla/2}\right) + 1\right].$$

Perturbation (Problem 1)

P1

advected perturbation :

$$\left\{\begin{aligned} \delta S &= \epsilon \cos\left(-\omega_0 t + k_x x + k_z z\right), \\ \frac{\delta\rho}{\rho_{\rm in}} &= \exp\left(-\frac{\gamma-1}{\gamma}\delta S\right) - 1, \\ \delta v_x &= \frac{k_x \omega_0}{\omega_0^2 + k_x^2 v_{\rm in}^2}\frac{c_{\rm in}^2}{\gamma}\delta S, \\ \delta v_z &= -\frac{k_x^2 v_{\rm in}}{\omega_0^2 + k_x^2 v_{\rm in}^2}\frac{c_{\rm in}^2}{\gamma}\delta S. \end{aligned}\right.$$

where $k_x = \dfrac{2\pi}{L_x}$ and $k_z = \dfrac{\omega_0}{v_{\rm in}}$

Movie (Problem 1)

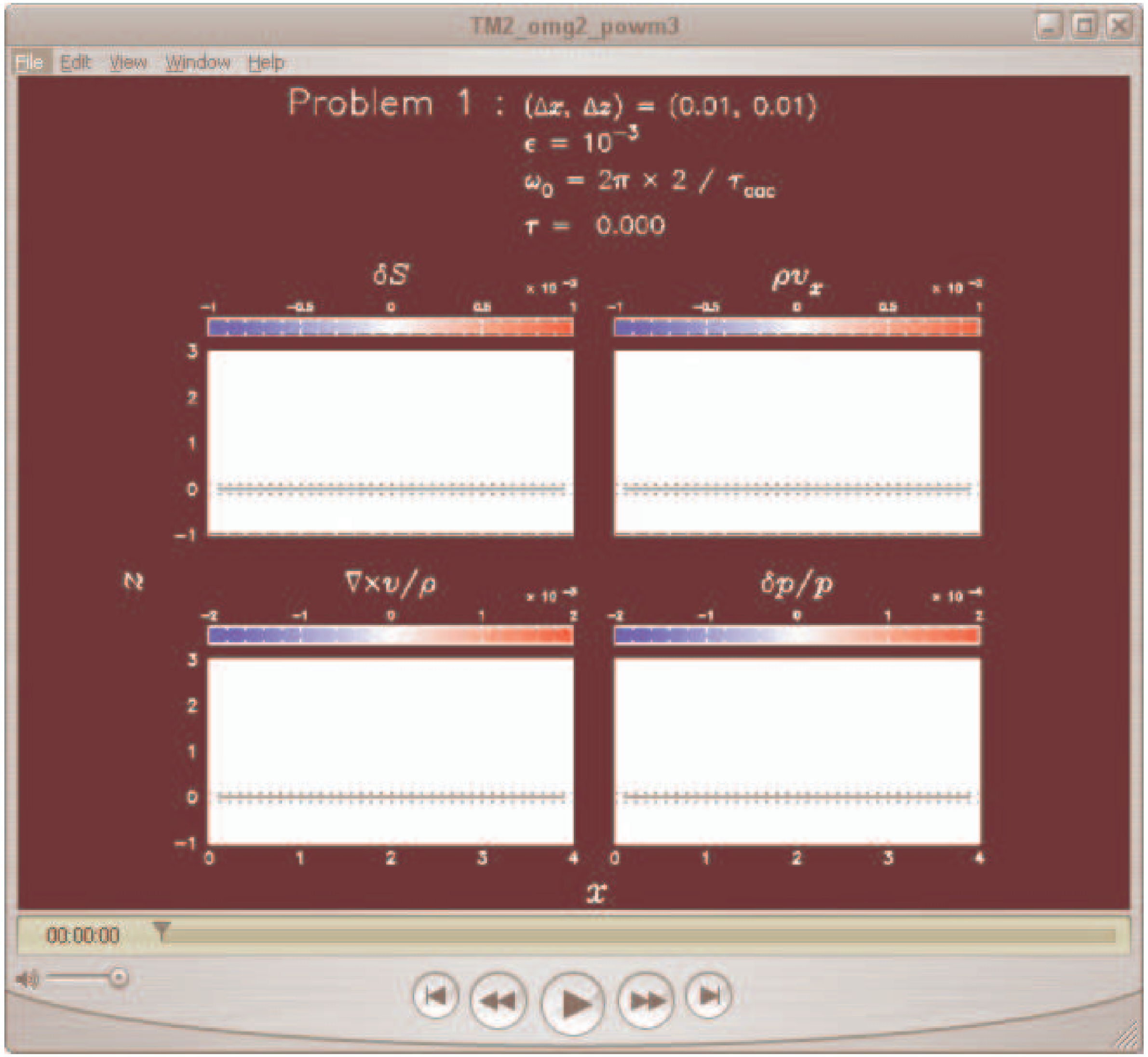

Snap Shots (Problem 1)

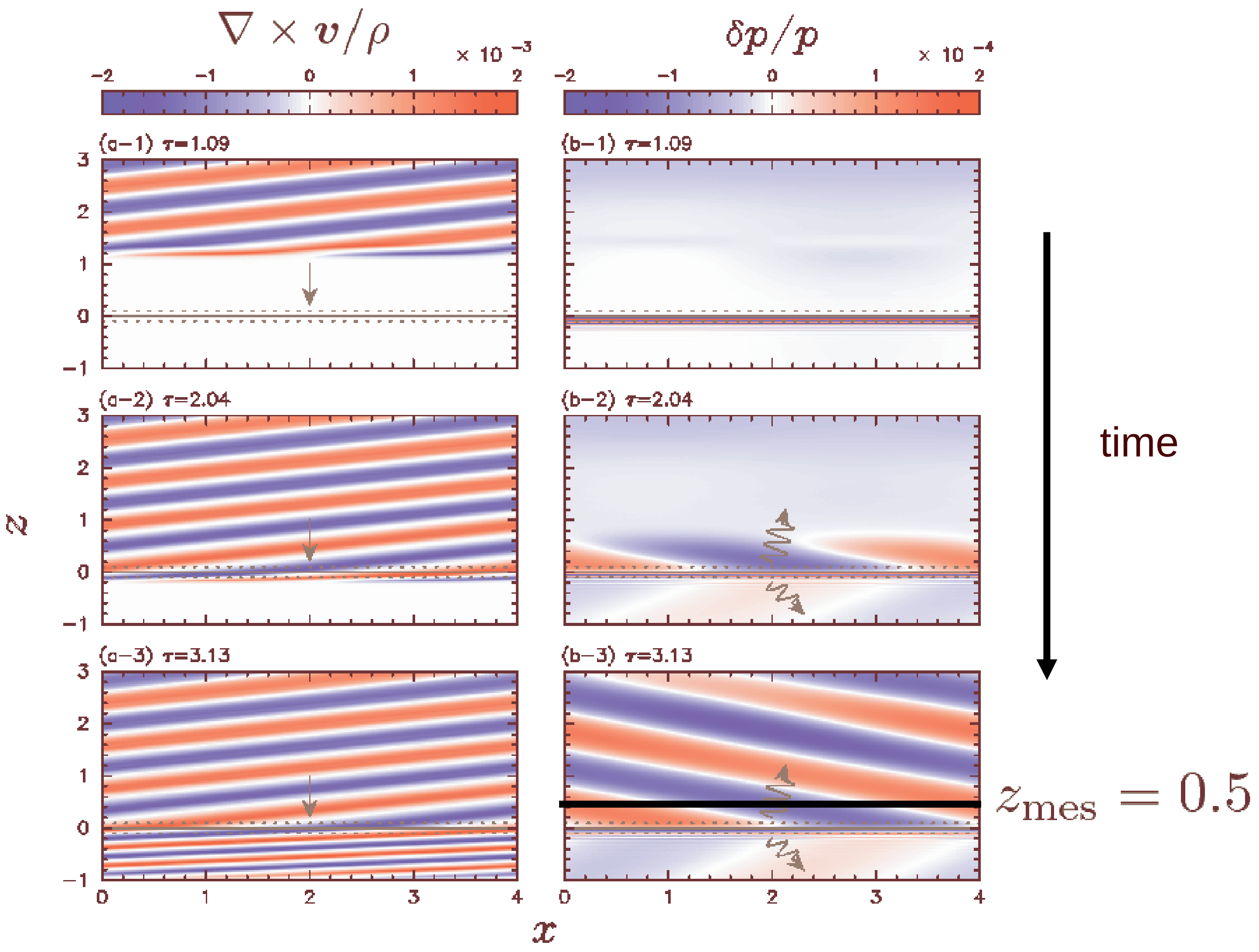

Prediction from linear analysis

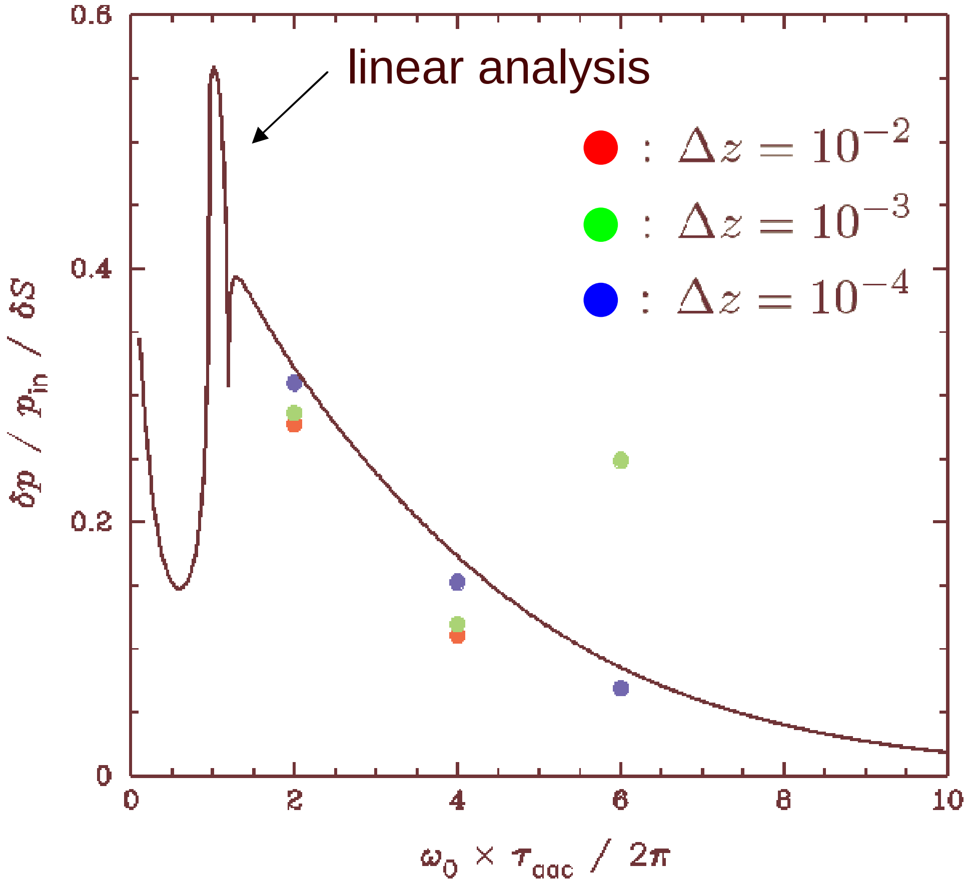

$$\begin{cases} \epsilon = 10^{-3} \\ \omega_0 = \dfrac{2\pi \times 2}{\tau_{\rm aac}}, \dfrac{2\pi \times 4}{\tau_{\rm aac}}, \dfrac{2\pi \times 6}{\tau_{\rm aac}} \end{cases}$$

where

$$\tau_{\rm aac} = \frac{1}{c_{\rm in}} \frac{1}{\mathcal{M}_{\rm in}(1-\mathcal{M}_{\rm in})}$$

- Our simulations with Δz=10^{-4}(=$10^{-3}\Delta z_{\nabla}$) in the linear phase can reproduce the linear analytical prediction very well.

Dependence on amplitude ϵ

We investigate the behavior of the toy model **in the non-linear phase** by increasing the perturbation amplitude ϵ.

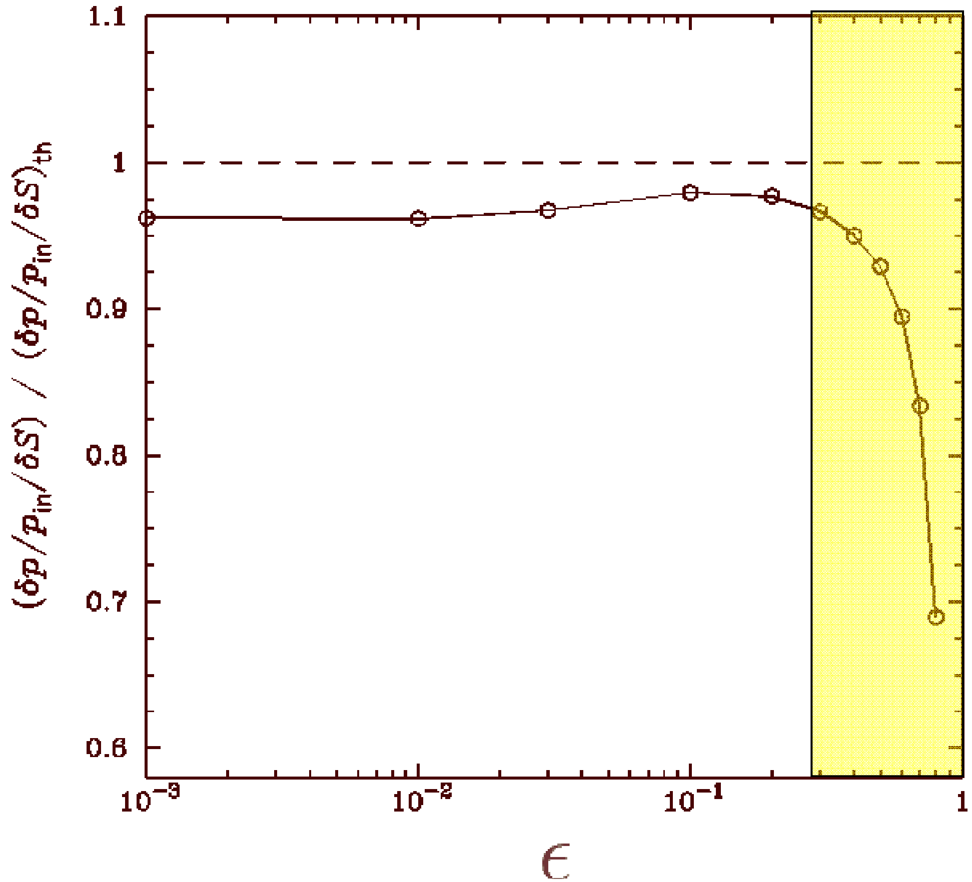

- The feed back efficiency begins to decrease at $\epsilon \sim 0.3$.
- Then the feed back efficiency decreases steeply with ϵ.

Problem 2 (in 1D)

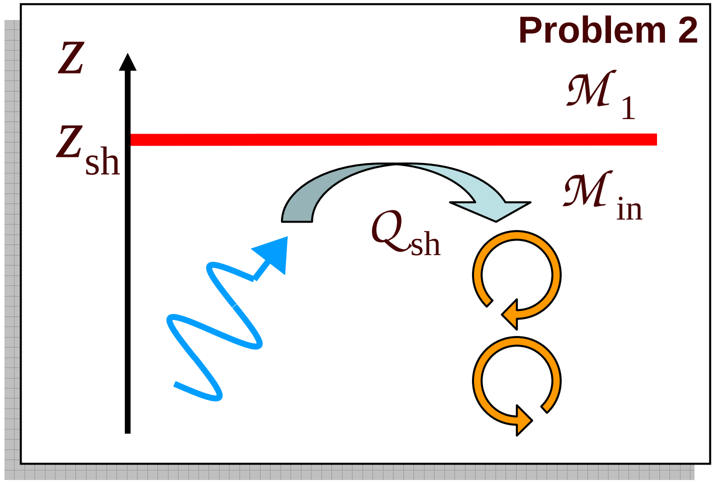

$$\Delta z = 10^{-2}, 10^{-3}, 10^{-4}$$

$$N_z = 394$$

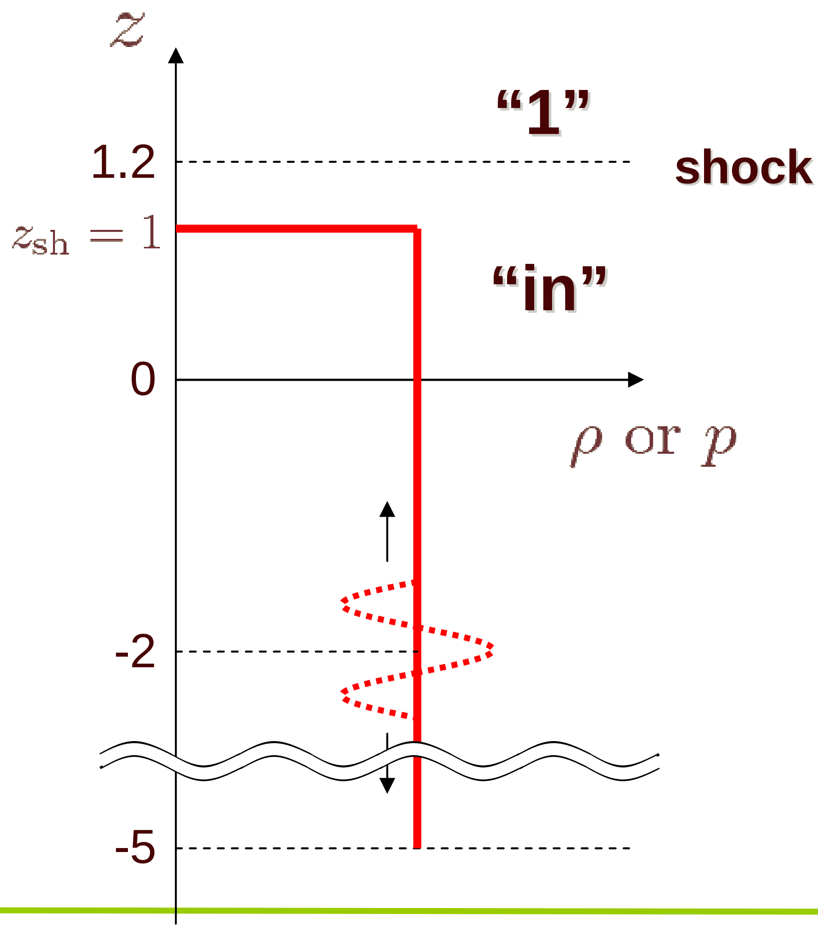

acoustic perturbation :

$$\frac{\delta\rho}{\rho_{\rm in}} = \frac{1+\mathcal{M}_{\rm in}}{1+\mathcal{M}_{\rm in}^2} \times \epsilon \cos(-\omega_0 t + k_z z)$$

$$\frac{\delta p}{p_{\rm in}} = \left(1 + \frac{\delta\rho}{\rho_{\rm in}}\right)^\gamma - 1,$$

where $\epsilon = 10^{-3}$

$$\omega_0 = \frac{2\pi \times 2}{\tau_{\rm aac}}, \frac{2\pi \times 4}{\tau_{\rm aac}}, \frac{2\pi \times 6}{\tau_{\rm aac}}$$

Temporal evolution of $\delta S/\delta S_{\rm th}$

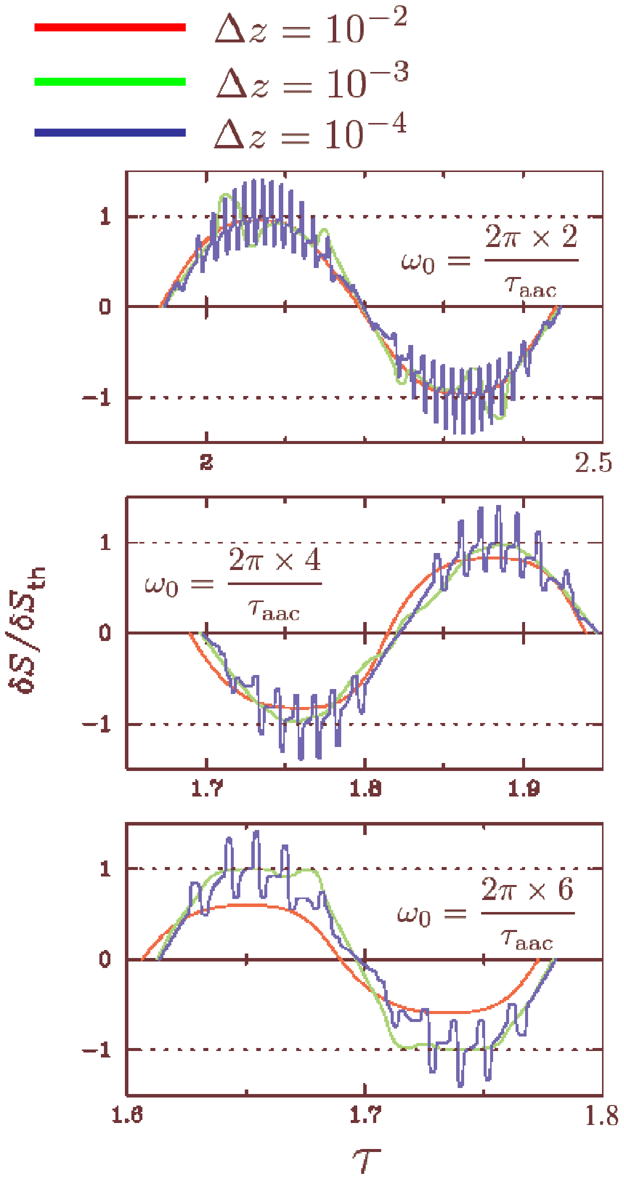

advected feed back predicted by linear analysis :

$$\delta S_{\rm th} = \frac{\delta p}{p_{\rm in}}\frac{2}{\mathcal{M}_{\rm in}}\frac{1-\mathcal{M}_{\rm in}^2}{1+\gamma\mathcal{M}_{\rm in}^2}\left(1-\frac{\mathcal{M}_{\rm in}^2}{\mathcal{M}_1^2}\right)\times\frac{\mu}{\mu^2+2\mu\mathcal{M}_{\rm in}+\mathcal{M}_1^{-2}}.$$

- In the high resolution simulations, the entropy wave generated at the shock contains **spurious high frequencies**.
- This is **a numerical artifact** associated with **postshock oscillations**.

Postshock oscillation is generated when the shock moves slowly with respect to the grid. (Colella & Woodward 1984; Jin & Liu 1996; Blondin et al. 2003; Stiriba & Donat 2003)

Power $|a_n|^2$ of $\delta S/\delta S_{\rm th}$

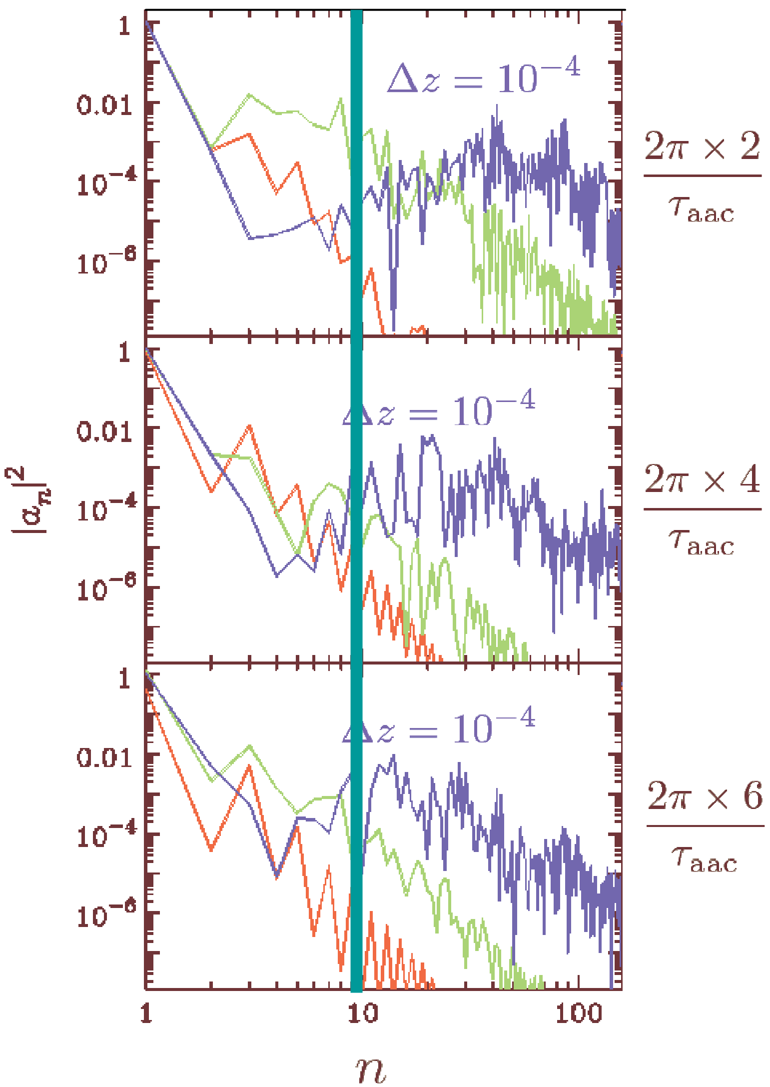

Fourier Transform :

$$|a_n|^2 = \left| \frac{2}{T} \int_0^T \frac{\delta S}{\delta S_{\rm th}} e^{i\omega_0 n t} dt \right|^2$$

- $\delta S/\delta S_{\rm th}$ in the simulations with the higher resolutions contains **higher frequency components**.
- In the simulation with the highest resolution, **$|a_{10}|^2$ achieves around 1%**.

  (*g*-mode frequency is 10 times higher than SASI frequency.)
- Could it contribute to ***g*-mode excitation?** This is unlikely, the energy seems negligible.

Dependence of $|a_1|^2$ on Δz

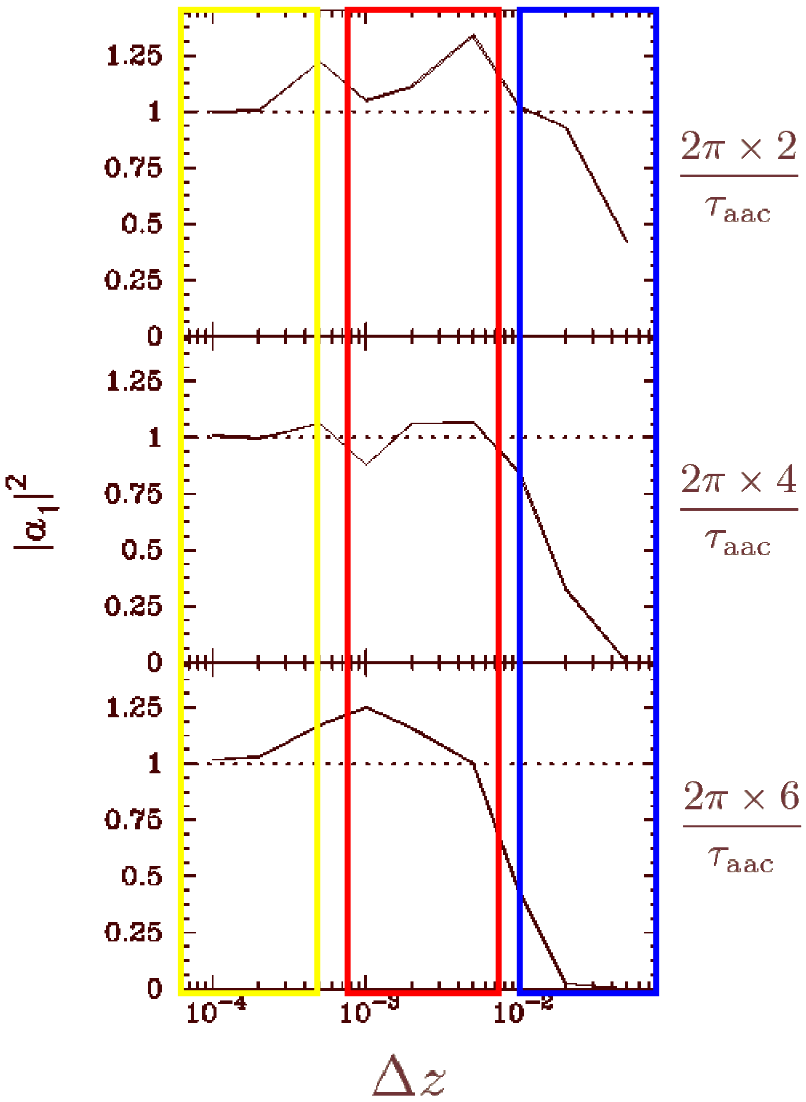

- At the highest resolution, **$|a_1|^2$ obtained from the simulation converges to ∼1.**
- **A very coarse resolution** in the linear phase **underestimates** the entropy production.
- **A moderately coarse resolution** in the linear phase can **overestimate** the entropy production by 25%.

Distribution of accuracy for $|a_1|^2$ *P2*

- The numerical treatment of the advective-acoustic coupling at the shock is controlled by the grid size Δz compared to **a advection wavelength λ_{adv}** and **a shock displacement $\Delta\zeta$**.

advection wavelength :

$$\lambda_{\mathrm{adv}} = \frac{2\pi|v_{\mathrm{in}}|}{\omega_0}$$

shock displacement :

$$\Delta\zeta = \left|\frac{c_{\mathrm{in}}^2}{v_1}\frac{\delta S}{\gamma}\frac{1}{(1-v_{\mathrm{in}}/v_1)^2}\frac{1}{\omega_0}\right|.$$

- due to the shock, 5% accuracy requires:

$$\frac{\lambda_{\mathrm{adv}}}{\Delta z} \geq 100$$

$$\frac{\Delta\zeta}{\Delta z} \geq 0.1$$

1D simulation

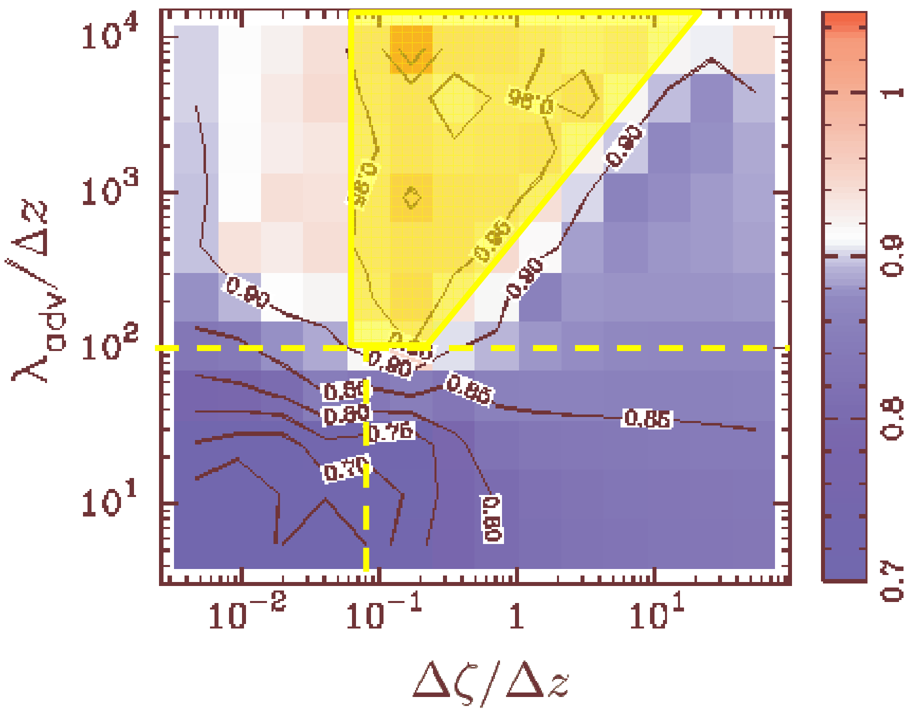

Grid size estimates in published simulations

P2

We estimate $\lambda_{\rm adv}/\Delta z$ in some published simulations.

advection wavelength : $\lambda_{\rm adv} = \frac{2\pi|v_{\rm in}|}{\omega_0}$

- $r_{\rm sh} = 1$
- ω_0 ←the oscillation frequency of $\ell = 1$ (the most unstable mode)
- $|v_{\rm in}| \sim \frac{\gamma - 1}{\gamma + 1} \times |v_{\rm ff}| = \frac{1}{7}|v_{\rm ff}|$
- We use the grid size at the shock position as Δz.

For example, Blondin et al. (2003)

N_r \ $r_{\rm sh}/r_*$	2	3.3	5	10
300	**206.4**	**196.0**	**166.4**	**149.6**
450	**230.2**	**215.0**	**182.4**	**160.9**

Grid size estimates in published simulations

Blondin & Mezzacappa (2006)

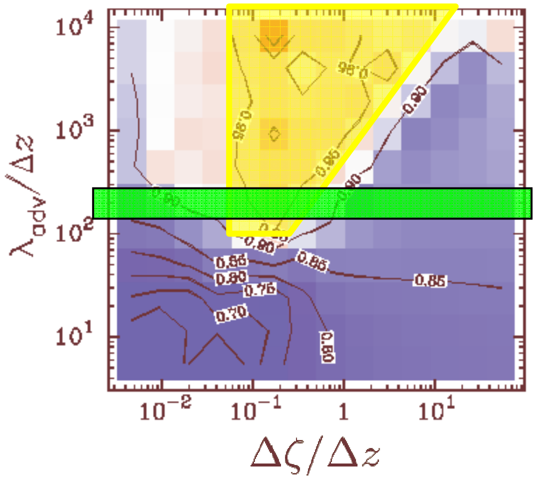

Ohnishi et al. (2006)

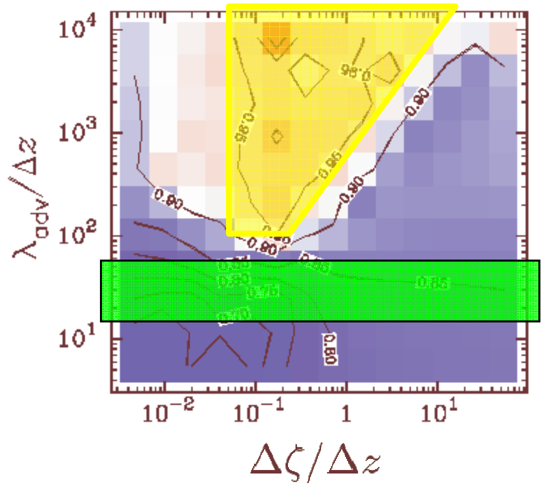

Scheck et al. (2008)

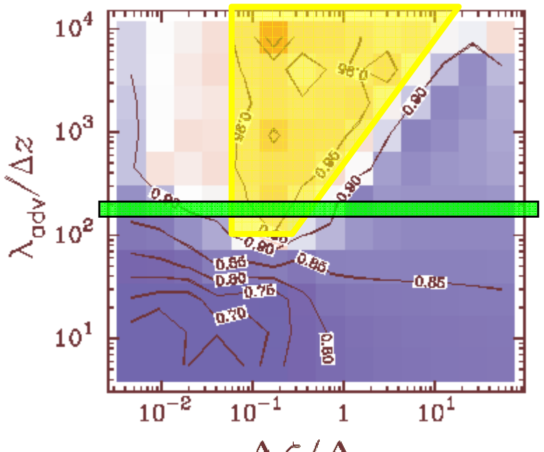

Burrows et al. (2006)

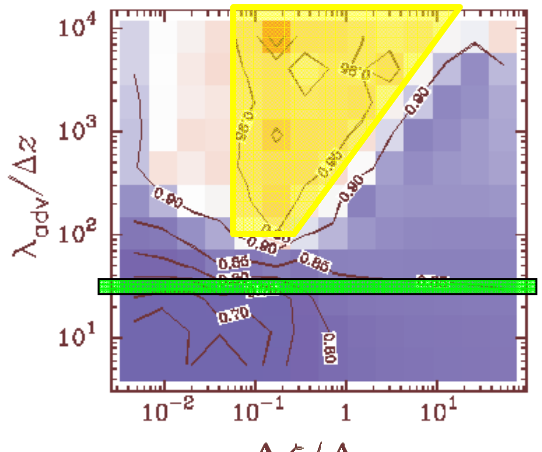

- This is only an estimate of the possible numerical error.
- But of course, this depends on numerical scheme.

Convergence

P2

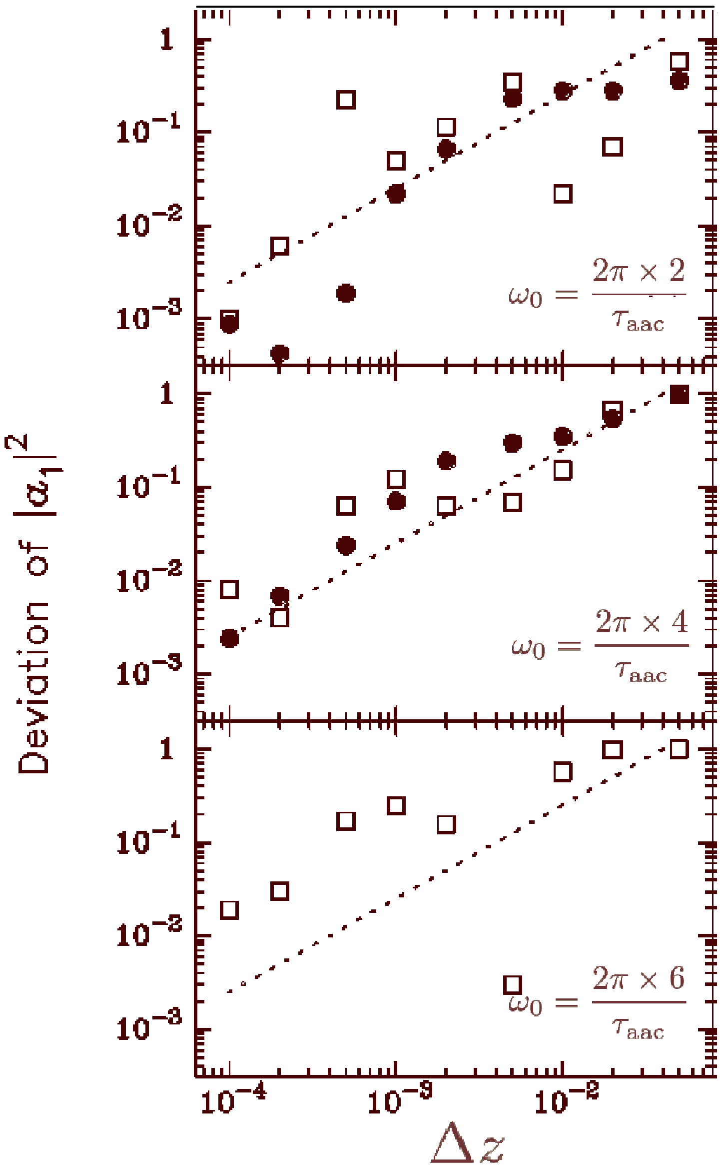

□ : AUSMDV scheme

- Although the points fluctuate, the deviation **almost linearly** decreases with decrease of Δz.

● : HLL scheme

(presented S. Fromang.
Refer to Londrillo & Del Zanna L 2004)

- The accuracy is **first order** for both numerical schemes.
- **The presence of the shock** reduces the accuracy to **first order**.

Problem 2

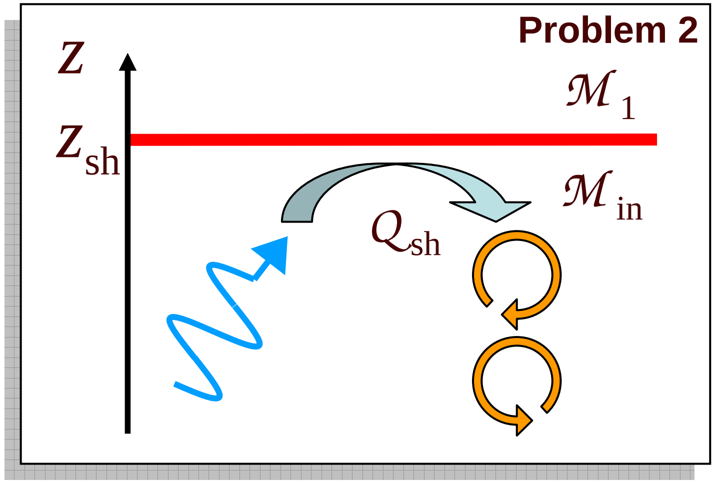

$$\Delta x = 10^{-2} \longrightarrow N_x = 400$$
$$\Delta z = 10^{-2} \longrightarrow N_z = 394$$

acoustic perturbation :

$$\frac{\delta\rho}{\rho_{\rm in}} = \frac{\mu + \mathcal{M}_{\rm in}}{1 - \mathcal{M}_{\rm in}^2} \times \epsilon \cos\left(-\omega_0 t + k_x x + k_z z\right),$$
$$\frac{\delta p}{p_{\rm in}} = \left(1 + \frac{\delta\rho}{\rho_{\rm in}}\right)^{\gamma} - 1,$$

where

$$\mu = \left[1 - \frac{k_x^2 c_{\rm in}^2}{\omega_0^2}\left(1 - \mathcal{M}_{\rm in}^2\right)\right]^{\frac{1}{2}}.$$

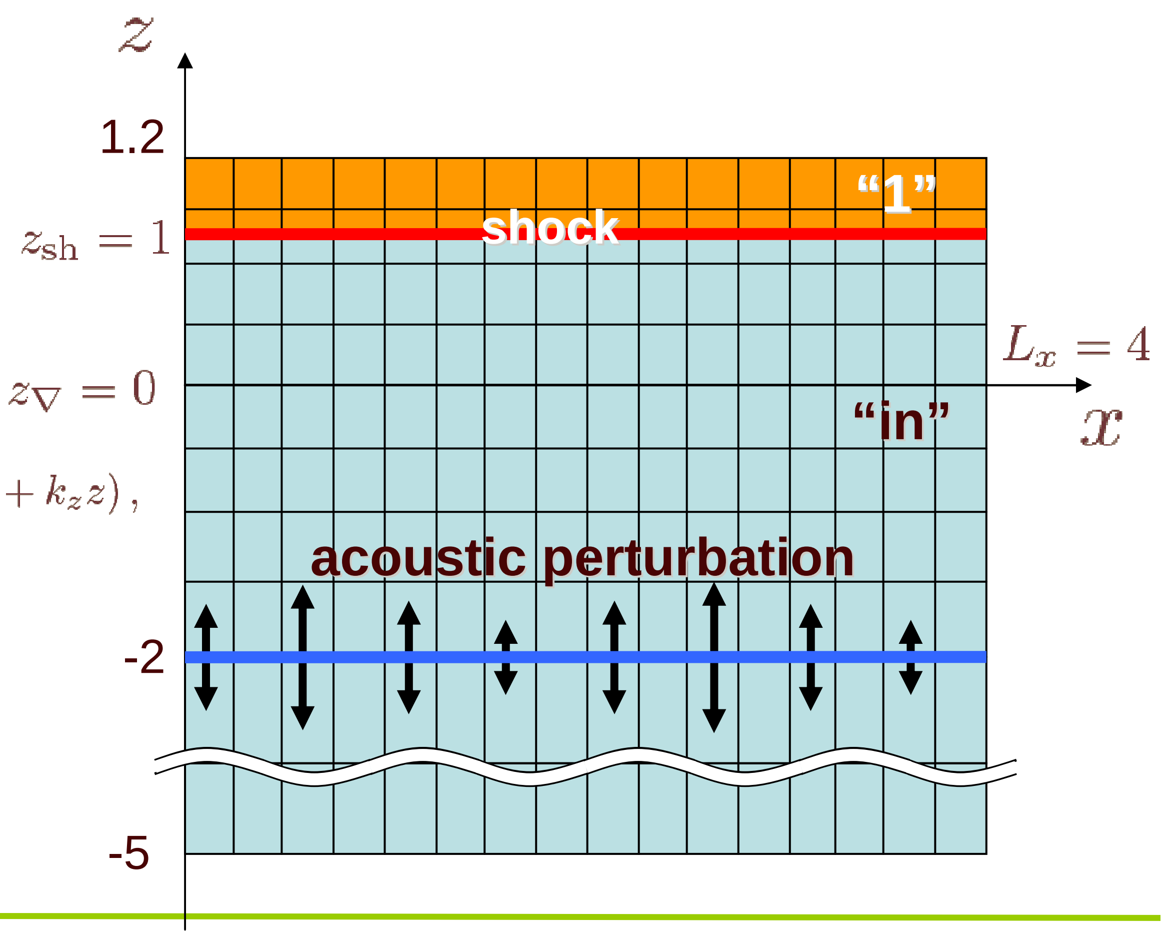

Movie (Problem 2 in 2D)

P2

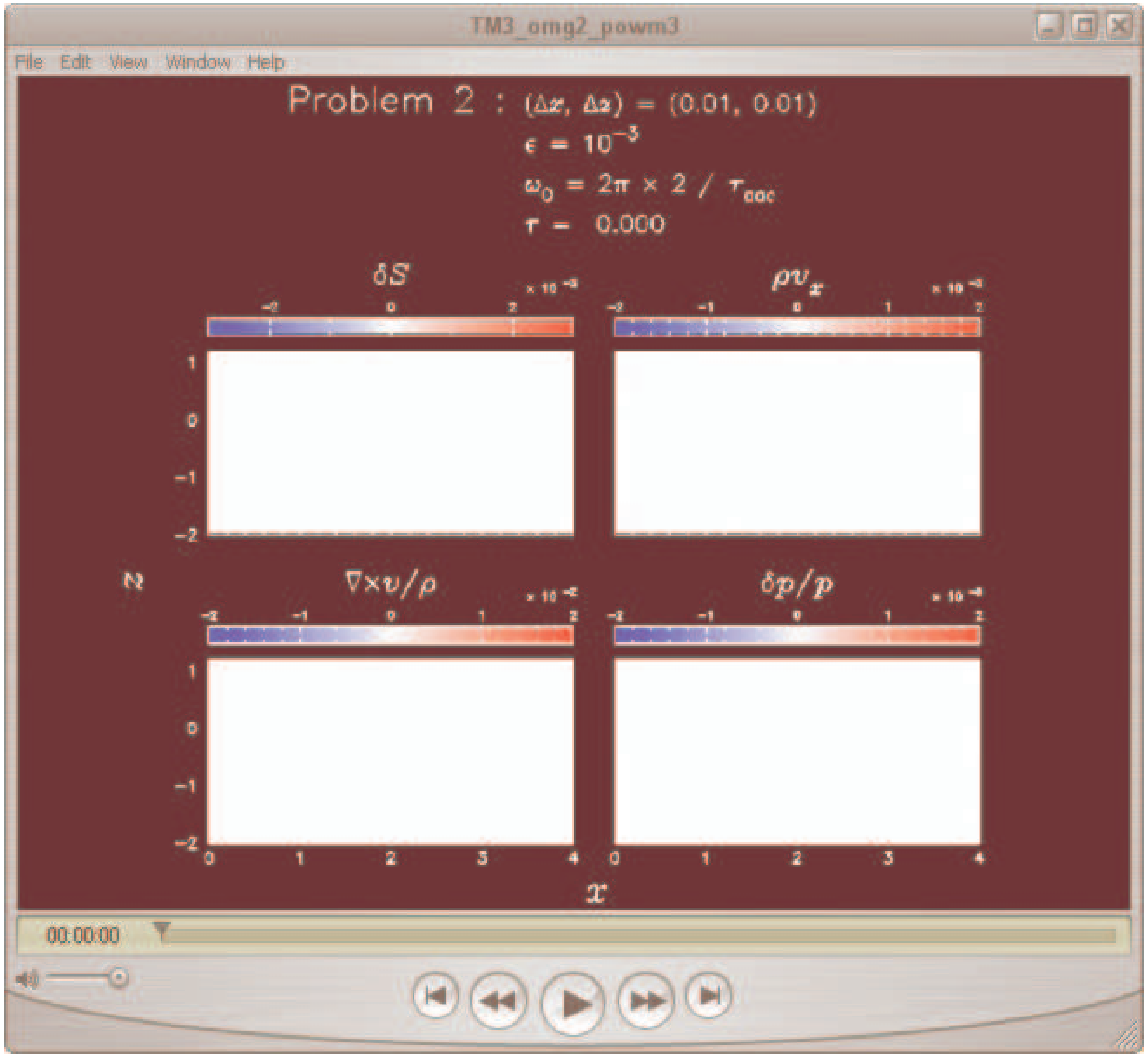

Conclusions

We performed the numerical simulations of the toy model which produces acoustic and advected feed back.

From problem 1

- The simulation with **small enough grid size** can reproduce the acoustic feed back predicted from the linear theory.
- We discovered that **the acoustic feed back decreases in the non-linear phase**.

From problem 2

- The coarse resolution can **overestimate** the entropy production by 25%.
- To reproduce the advective feed back, **the grid size of ∼1/1000 of the shock distance** is needed.
- The reason is that including the shock reduces the accuracy of the simulation to **first order**.
- **The postshock oscillation** produces spurious high frequency oscillations in the advected wave.
- However, the energy leak involved is 1% or less, and it is small enough and **probably doesn't influence *g*-mode excitation**.

Future work

1. The toy model can address the question of **the horizontal momentum transfer** in SASI mechanism.

   ⇒ the problem of pulsar spin

2. We try to perform the simulation of **the complete toy model**.

   ⇒ a benchmark test

   ⇒ non-linear phase of the toy model